Beyond Gaussianity: Extending the Clustering–Recovery Bridge

Lluis Eriksson
Independent Researcher
lluiseriksson@gmail.com

December 31, 2025

Abstract

We formulate a non-Gaussian, finite-volume and uniform-in-Λ version of the Clustering–Recovery bridge for interacting lattice systems. We introduce an explicit collar geometry, a CMI formulation via Fawzi–Renner [1], and an operational (Heisenberg-picture) quasi-locality strengthening for the recovery map.

1 Beyond Gaussianity: extending the Clustering–Recovery bridge

The proof strategy used in the Gaussian setting relies crucially on the quasi-free structure: all correlation data are encoded in the two-point function and the recovery map can be built from linear (symplectic) transformations. In interacting theories such a reduction is not available. This motivates the following program: replace Gaussian structure by *robust, model-independent* notions of clustering and quasi-locality, and derive recoverability (or small conditional mutual information) from these assumptions using genuinely non-Gaussian techniques.

1.1 Working framework and notions of clustering

We consider a lattice system with finite-dimensional local Hilbert spaces, so that finite-region restrictions are described by density matrices. Throughout this section we work with a family of finite-volume states $(\rho_\Lambda)_\Lambda$ (e.g. finite-volume Gibbs states for a finite-range interaction with a fixed choice of boundary conditions). All bounds are required to hold uniformly in Λ.

For each finite volume Λ, let $\mathrm{dist}(\cdot,\cdot)$ denote the graph distance induced by Λ (with the chosen boundary conditions). Given regions $X, Y \subseteq \Lambda$, we denote by $\mathrm{dist}(X,Y)$ their graph distance, i.e.,

$$\mathrm{dist}(X,Y) := \min\{\mathrm{dist}(x,y) : x \in X,\ y \in Y\}. \tag{1}$$

We also use the point-to-set distance

$$\mathrm{dist}(x,A) := \min\{\mathrm{dist}(x,y) : y \in A\}. \tag{2}$$

Correlations are quantified through connected correlators (a.k.a. truncated correlations).

Definition 1 (Connected correlator and uniform exponential clustering)**.** *Let ρ_Λ be a finite-volume state on Λ and let O_X and O_Y be observables supported on regions X and Y. The connected correlator is*

$$\mathrm{Corr}_{\rho_\Lambda}(O_X,O_Y) := \mathrm{Tr}(\rho_\Lambda\, O_X O_Y) - \mathrm{Tr}(\rho_\Lambda\, O_X)\mathrm{Tr}(\rho_\Lambda\, O_Y). \tag{3}$$

We say that the family $(\rho_\Lambda)_\Lambda$ has uniform exponential clustering *if there exist constants $c, \xi > 0$ such that for all volumes Λ, all disjoint $X, Y \subseteq \Lambda$, and all observables O_X, O_Y with $\|O_X\|_\infty, \|O_Y\|_\infty \le 1$,*

$$\left|\mathrm{Corr}_{\rho_\Lambda}(O_X,O_Y)\right| \le c\, e^{-\mathrm{dist}(X,Y)/\xi}. \tag{4}$$

In the interacting case, Definition 1 is a minimal replacement; however, for entropic statements (recoverability/CMI) one typically needs *uniform* bounds that are stable under conditioning on a buffer region and/or higher-order cumulant control (see Section 1.5).

1.2 Geometric setup: a collar buffer of width w

Let Λ be a finite region and let $A \subset \Lambda$ be a subregion. For an integer $w \geq 1$, define the w-neighborhood

$$A^{(w)} := \{x \in \Lambda : \mathrm{dist}(x, A) \leq w\}, \tag{5}$$

and set

$$B := A^{(w)} \setminus A, \qquad C := \Lambda \setminus A^{(w)}. \tag{6}$$

Then A, B, C are disjoint and B is a separating collar of width w between A and C.

If Λ has open boundary conditions, we restrict to an *admissible class* of regions A such that

$$\mathrm{dist}(A, \partial\Lambda) \geq w, \tag{7}$$

so that the collar does not intersect the boundary. For torus boundary conditions, no such restriction is needed.

1.3 A non-Gaussian extension of Conjecture 5.1

We take fidelity in the Uhlmann form

$$F(\rho, \sigma) := \|\sqrt{\rho}\sqrt{\sigma}\|_1^2. \tag{8}$$

Conjecture 1 (General Clustering–Recovery bridge beyond Gaussianity)**.** *Assume $(\rho_\Lambda)_\Lambda$ has uniform exponential clustering as in Definition 1 with correlation length ξ. For any finite volume Λ, any admissible region $A \subseteq \Lambda$, and any collar width $w \geq 1$, consider the induced collar tripartition A, B, C defined in (5)–(6), and let ρ_{ABC} and ρ_{AB} denote the corresponding reduced density matrices of ρ_Λ.*

Then there exist constants $c', \alpha > 0$ (depending only on microscopic locality data and ξ, and not on Λ, A, or w) such that for each choice of (Λ, A, w) there exists a recovery channel $\mathcal{R}_{B\to BC}$. Here $\mathcal{R}_{B\to BC}$ is a CPTP map acting nontrivially only on subsystem B and satisfying

$$1 - F(\rho_{ABC}, (\mathrm{id}_A \otimes \mathcal{R}_{B\to BC})(\rho_{AB})) \leq c'\, e^{-\alpha\, w/\xi}. \tag{9}$$

Remark 1 (Locality of dynamics vs locality of recovery)**.** *In interacting systems, locality of the interaction typically yields Lieb–Robinson bounds [2], but quasi-locality of recovery is not automatic. The conjecture above is therefore complemented by the optional operational strengthening below.*

Optional strengthening (operational quasi-locality of recovery). One may further conjecture a *quasi-local* form of recovery formulated in the Heisenberg picture. Let $\mathcal{R}^\dagger_{B\to BC}$ denote the adjoint channel on observables. There exist $c_{\mathrm{ql}}, \alpha_{\mathrm{ql}} > 0$ such that for any region $C_0 \subseteq C$ with $\mathrm{dist}(C_0, B) \geq r$ and any observable O_{C_0} with $\|O_{C_0}\|_\infty \leq 1$, where $\rho_{C_0} := \mathrm{Tr}_{\Lambda\setminus C_0}(\rho_\Lambda)$ denotes the reduced state on C_0,

$$\left\| \mathcal{R}^\dagger_{B\to BC}(O_{C_0}) - \mathrm{Tr}(\rho_{C_0} O_{C_0})\, \mathbf{1}_B \right\|_\infty \leq c_{\mathrm{ql}} e^{-\alpha_{\mathrm{ql}} r/\xi}. \tag{10}$$

Entropic conventions (finite-dimensional). For a finite-dimensional density matrix ρ we use the von Neumann entropy and quantum relative entropy

$$\begin{aligned} S(\rho) &:= -\mathrm{Tr}(\rho \log \rho), \\ D(\rho\|\sigma) &:= \mathrm{Tr}\big(\rho(\log \rho - \log \sigma)\big), \end{aligned} \tag{11}$$

with $D(\rho\|\sigma) = +\infty$ if $\mathrm{supp}(\rho) \not\subseteq \mathrm{supp}(\sigma)$.

For a tripartite state ρ_{ABC}, the conditional mutual information (CMI) is

$$I(A:C|B)_{\rho_{ABC}} := S(\rho_{AB}) + S(\rho_{BC}) - S(\rho_B) - S(\rho_{ABC}). \tag{12}$$

1.3.1 CMI formulation via Fawzi–Renner

A slightly weaker, and often more accessible, formulation replaces explicit recoverability by a bound on conditional mutual information (CMI). Applied to the finite-dimensional state ρ_{ABC}, the Fawzi–Renner inequality [1] implies that there exists a channel $\mathcal{R}_{B\to BC}$ such that

$$I(A:C|B)_{\rho_{ABC}} \geq -2 \log F(\rho_{ABC},\, (\mathrm{id}_A \otimes \mathcal{R}_{B\to BC})(\rho_{AB}))\,. \tag{13}$$

Thus, a sufficient route to Conjecture 1 is to prove an exponential decay estimate

$$I(A:C|B)_{\rho_{ABC}} \leq c'' e^{-\alpha w/\xi}, \tag{14}$$

and then convert it to an explicit recovery-fidelity bound via the inequality above.

CMI as relative entropy (finite-volume, support-aware). For intuition, one may represent CMI as a relative entropy to a (normalized) "Markov product" state:

$$I(A:C|B)_{\rho_{ABC}} = D\Big(\rho_{ABC} \,\Big\|\, \sigma^{\mathrm{MP}}_{ABC}\Big)\,, \tag{15}$$

with

$$\sigma^{\mathrm{MP}}_{ABC} := \frac{\exp(\log \rho_{AB} + \log \rho_{BC} - \log \rho_B)}{\mathrm{Tr}\exp(\log \rho_{AB} + \log \rho_{BC} - \log \rho_B)}. \tag{16}$$

1.4 Why Gaussian proofs do not port, and what to replace them with

In the Gaussian case, the recovery map is effectively determined by the two-point data and the proof is a matrix-analysis problem. In interacting models, none of the following hold in general:

1. Wick reduction of higher correlators to two-point functions,
2. linear/symplectic structure of an optimal recovery channel,
3. closed-form expressions for entropies and CMI in terms of finitely many correlators.

Hence the extension requires techniques that (a) connect *correlator clustering* to *entropic* statements, and (b) construct (or certify existence of) a *quasi-local* recovery map.

1.5 Technical tool-kit needed outside Gaussian structure

Below is a concrete list of candidate ingredients that can replace Gaussian linear algebra.

1. **Quasi-locality bounds (Lieb–Robinson type).** [2]
2. **Gapped ground states and exponential clustering.** [3]

3. **Approximate factorization / buffer decoupling.**

$$\|\rho_{AC} - \rho_A \otimes \rho_C\|_1 \leq c\, e^{-\mathrm{dist}(A,C)/\xi}. \tag{17}$$

4. **From clustering of correlators to clustering of relative entropy / CMI.**

5. **Cluster expansion / polymer methods (high temperature, weak coupling).** [4]

6. **Approximate quantum Markov chains and recovery (Petz / rotated Petz).** [1, 5, 6]

$$\mathcal{R}^t_{B\to BC}(X) := \rho_{BC}^{\frac{1+it}{2}}\, \rho_B^{-\frac{1+it}{2}}\, X\, \rho_B^{-\frac{1-it}{2}}\, \rho_{BC}^{\frac{1-it}{2}}. \tag{18}$$

7. **Modular flow locality (approximate) and Araki-type bounds.**

8. **Cumulant control beyond two-point functions.**

$$|\kappa_k(O_{X_1}, \ldots, O_{X_k})| \leq c_k\, \exp\Big(-\mathrm{TreeDist}(X_1, \ldots, X_k)/\xi\Big). \tag{19}$$

2 Numerical experiments (Colab): TFIM Gibbs recovery

Why numerics here. A complete analytical proof of Conjecture 1 in interacting lattice systems would require assembling several non-Gaussian ingredients (Section 1.5), including conditional versions of clustering and a controlled route from correlator decay to entropic quantities such as $I(A:C|B)$. Pending such a full theory, we provide finite-size numerical evidence in a paradigmatic interacting model (the 1D TFIM Gibbs state) and directly test the predicted exponential-in-buffer-width behavior of recovery errors for explicit candidate maps (Petz and averaged rotated-Petz).

2.1 Numerical methodology (model, partition, recovery maps, and fits)

Model and Gibbs state. We consider the transverse-field Ising chain with open boundary conditions

$$H = -J \sum_{i=1}^{N-1} X_i X_{i+1} - h \sum_{i=1}^{N} Z_i, \tag{20}$$

and the Gibbs state $\rho \propto e^{-\beta H}$ computed by exact diagonalization in finite dimension. In the runs reported below we fix $N = 10$ and $J = 1$ and sweep $h \in \{1.05, 1.10, 1.20, 1.50\}$ and $\beta \in \{0.3, 0.6, 1.0, 1.5, 2.0\}$.

Collar partition used in the numerics. To match the CSV/PNG artifacts exported by the Colab pipeline, we use the 1D collar tripartition

$$A = \{1, \ldots, L_A\}, \quad B = \{L_A + 1, \ldots, L_A + w\}, \quad C = \{L_A + w + 1, \ldots, N\}, \tag{21}$$

with $L_A = 2$ and $w \in \{1, \ldots, 6\}$.

Remark on admissibility. The admissibility condition (7) is introduced to state the conjecture in a boundary-robust form for general finite volumes. In the present finite 1D benchmark we do not impose (7) (for large w the collar meets the boundary), and we treat the results as controlled finite-size evidence for the qualitative w-dependence of recovery errors.

CMI and recovery. For each (h, β, w) we compute the reduced states ρ_{AB}, ρ_B, ρ_{BC}, and ρ_{ABC} by partial tracing. We compute $I(A:C|B)$ from von Neumann entropies. For each recovery method $\mathcal{R}_{B\to BC}$ we form the reconstructed state

$$\tilde{\rho}_{ABC} := (\mathrm{id}_A \otimes \mathcal{R}_{B\to BC})(\rho_{AB}). \tag{22}$$

In finite dimension, the Petz map is implemented in the standard form

$$\mathcal{R}^{\mathrm{Petz}}_{B\to BC}(X) = \rho_{BC}^{1/2}\Big(\rho_B^{-1/2} X \rho_B^{-1/2} \otimes \mathbf{1}_C\Big)\rho_{BC}^{1/2}. \tag{23}$$

Here $\rho_B^{-1/2}$ is understood as the inverse on $\mathrm{supp}(\rho_B)$ (equivalently, via the Moore–Penrose pseudoinverse), so that $\mathcal{R}^{\mathrm{Petz}}_{B\to BC}$ is a completely positive trace-preserving map in exact arithmetic. In the numerics we apply the spectral regularization described below. For the rotated-Petz method we use a discretized averaged map $\mathcal{R}^{\mathrm{rot}}_{B\to BC} \approx \sum_k w_k \mathcal{R}^{t_k}_{B\to BC}$ with $w_k \geq 0$ and $\sum_k w_k = 1$, so the implemented map is a convex combination of completely positive maps. The subsequent PSD-clipping and trace renormalization is a numerical post-processing step applied to $\tilde{\rho}_{ABC}$ (to ensure it is a valid density matrix); it is not claimed to preserve exact channel properties at the map level.

Regularization. When inverses or complex powers of ρ_B are required (Petz / rotated-Petz), we diagonalize $\rho_B = \sum_j \lambda_j |j\rangle\langle j|$ and implement all matrix functions on $\mathrm{supp}(\rho_B)$ with eigenvalue flooring: we replace λ_j by $\max\{\lambda_j, \varepsilon_{\mathrm{inv}}\}$ with $\varepsilon_{\mathrm{inv}} = 10^{-12}$ before applying λ_j^α (including $\alpha = -1/2$). After each reconstruction step we enforce Hermiticity and project to the PSD cone by clipping eigenvalues below $\varepsilon_{\mathrm{psd}} = 10^{-14}$, followed by trace renormalization.

Rotated-Petz averaging (discretized). We approximate the averaged rotated-Petz map by a truncated quadrature with $t \in [-t_{\max}, t_{\max}]$, $t_{\max} = 6$, using $n_t = 61$ uniform nodes and trapezoidal weights. Weights are taken proportional to $(\cosh(\pi t) + 1)^{-1}$ and normalized on the truncated grid, following the standard averaged rotated-Petz construction (see e.g. [6]). In implementation we explicitly normalize the discrete weights so that $\sum_k w_k = 1$ and $w_k \geq 0$, and we apply the resulting convex combination to obtain $\tilde{\rho}_{ABC}$ as in (22). Any small deviations from positivity or unit trace arising from spectral flooring and floating-point error are corrected by the PSD-clipping and trace renormalization step described above.

Error metrics. We report the trace distance

$$T(w) := \frac{1}{2}\|\rho_{ABC} - \tilde{\rho}_{ABC}\|_1, \tag{24}$$

and the Hilbert–Schmidt norm $\|\rho_{ABC} - \tilde{\rho}_{ABC}\|_2$. We also report $T(w)^2$ as a proxy motivated by the Fuchs–van de Graaf inequalities $T(w)^2 \leq 1 - F \leq 2T(w)$ (see e.g. [7]).

Exponential fits. For each observable $y(w)$ we fit $\log y(w) \approx a - \mu w$ over the sampled w range (least squares on positive data points) and report the fitted slope μ.

Reproducibility (artifacts). The Colab scripts export per-parameter curves (as CSV) and the derived summaries (slopes, crossover widths, and plots as PNG). The tables and figures below are direct renderings of those artifacts. The computations were carried out in a standard Google Colab environment (Python with NumPy/SciPy stack); exact package versions are recorded in the notebook output.

2.2 Fitted exponential slopes

We fit $y(w) \sim e^{a-\mu w}$ and report the fitted slopes μ.

2.3 Prefactor–slope trade-off and crossover widths

In the high-temperature regime, we observe a consistent prefactor–slope trade-off: rotated-Petz can yield smaller $T(w)$ at $w = 1$ while Petz typically exhibits a larger decay rate in w and overtakes at a modest crossover width $w^\star$.

Limitations. Our numerics are finite-size and focus on a specific 1D model and collar geometry. We do not claim thermodynamic-limit uniformity, nor do we provide certified uncertainty bars for fitted slopes beyond the finite grid and least-squares fitting procedure described above. The purpose is to provide controlled evidence for the qualitative prefactor–slope trade-off and the existence of a modest crossover width $w^\star$ in the tested regime.

References

[1] Omar Fawzi and Renato Renner. Quantum conditional mutual information and approximate markov chains. *Communications in Mathematical Physics*, 340(2):575–611, 2015.

[2] Elliott H. Lieb and Derek W. Robinson. The finite group velocity of quantum spin systems. *Communications in Mathematical Physics*, 28(3):251–257, 1972.

[3] Matthew B. Hastings and Toshihiro Koma. Spectral gap and exponential decay of correlations. *Communications in Mathematical Physics*, 265(3):781–804, 2006.

[4] Matthias Kliesch, Christian Gogolin, Michael J. Kastoryano, Alexander Riera, and Jens Eisert. Locality of temperature. *Physical Review X*, 4(3):031019, 2014.

[5] Dénes Petz. Sufficient subalgebras and the relative entropy of states of a von Neumann algebra. *Communications in Mathematical Physics*, 105:123–131, 1986.

[6] Marius Junge, Renato Renner, David Sutter, Mark M. Wilde, and Andreas Winter. Universal recovery maps and approximate sufficiency of quantum relative entropy. *Annales Henri Poincaré*, 19:2955–2978, 2018.

[7] Michael A. Nielsen and Isaac L. Chuang. *Quantum Computation and Quantum Information*. Cambridge University Press, 10th anniversary edition edition, 2010.

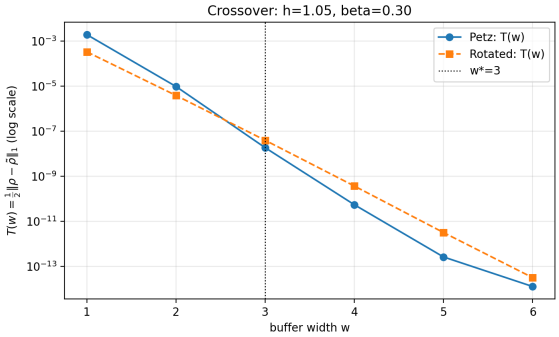

(a) $h = 1.05,\ \beta = 0.30$

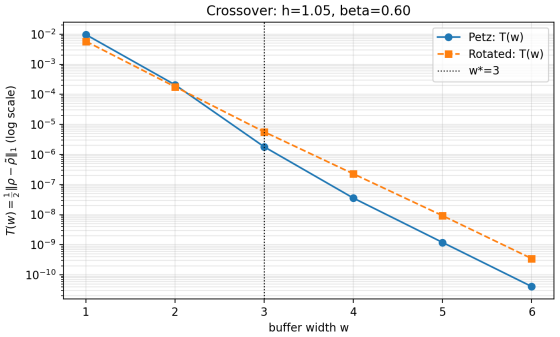

(b) $h = 1.05,\ \beta = 0.60$

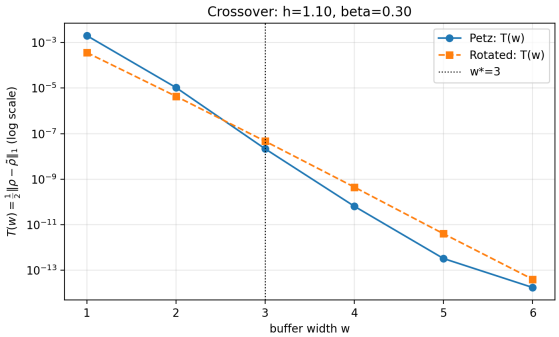

(c) $h = 1.10,\ \beta = 0.30$

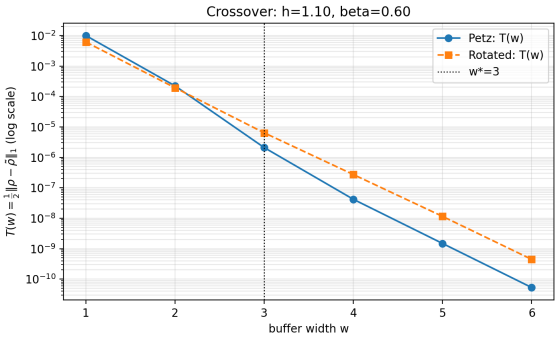

(d) $h = 1.10,\ \beta = 0.60$

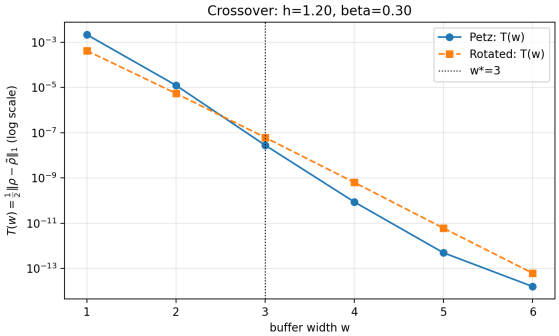

(e) $h = 1.20,\ \beta = 0.30$

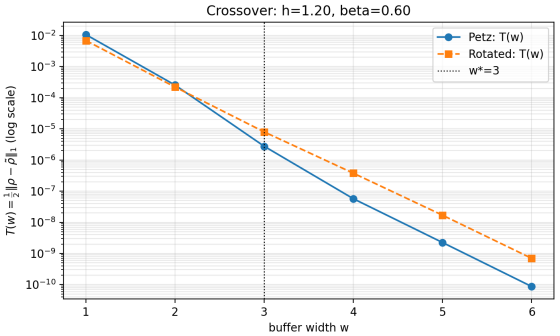

(f) $h = 1.20,\ \beta = 0.60$

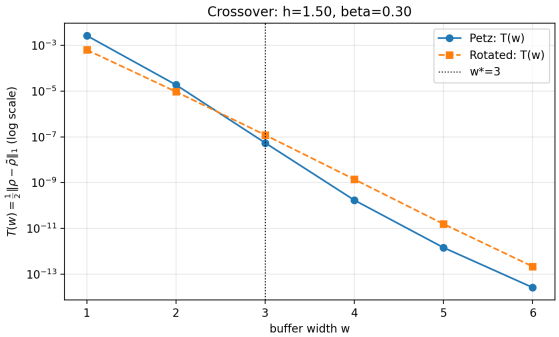

(g) $h = 1.50,\ \beta = 0.30$

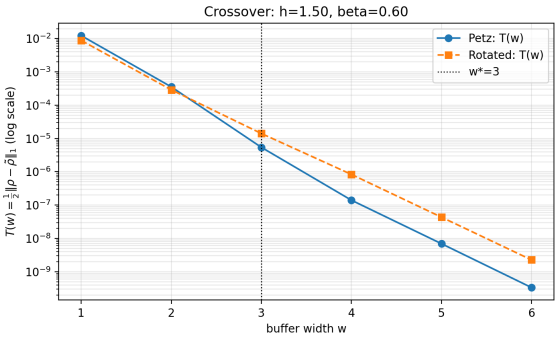

(h) $h = 1.50,\ \beta = 0.60$

Figure 1: Trace-distance recovery error $T(w) = \frac{1}{2}\|\rho_{ABC} - \tilde{\rho}_{ABC}\|_1$ versus buffer width w for the eight disagreement cases: rotated-Petz is better at $w = 1$ (prefactor), while Petz overtakes for $w \geq w^\star$ (slope).

N	L_A	h	β	method	μ_{CMI}	μ_T	μ_{HS}	μ_{T^2}
10	2	1.05	0.30	petz	7.0354	5.3352	5.3002	10.6705
10	2	1.05	0.30	rotated	7.0354	4.6294	4.6326	9.2587
10	2	1.05	0.60	petz	4.4807	3.8992	3.8466	7.7983
10	2	1.05	0.60	rotated	4.4807	3.3117	3.2917	6.6233
10	2	1.05	1.00	petz	3.0063	2.7623	2.7326	5.5246
10	2	1.05	1.00	rotated	3.0063	2.3692	2.3489	4.7383
10	2	1.05	1.50	petz	2.0991	2.0078	1.9949	4.0156
10	2	1.05	1.50	rotated	2.0991	1.7075	1.6920	3.4150
10	2	1.05	2.00	petz	1.6014	1.5659	1.5608	3.1317
10	2	1.05	2.00	rotated	1.6014	1.3064	1.2975	2.6128
10	2	1.10	0.30	petz	4.9396	5.2877	5.2121	10.5754
10	2	1.10	0.30	rotated	4.9396	4.5992	4.6008	9.1984
10	2	1.10	0.60	petz	4.4085	3.8551	3.8054	7.7102
10	2	1.10	0.60	rotated	4.4085	3.2721	3.2534	6.5442
10	2	1.10	1.00	petz	2.9533	2.7282	2.7040	5.4565
10	2	1.10	1.00	rotated	2.9533	2.3376	2.3198	4.6752
10	2	1.10	1.50	petz	2.0622	1.9797	1.9743	3.9593
10	2	1.10	1.50	rotated	2.0622	1.6825	1.6716	3.3651
10	2	1.10	2.00	petz	1.5756	1.5386	1.5428	3.0773
10	2	1.10	2.00	rotated	1.5756	1.2868	1.2834	2.5736
10	2	1.20	0.30	petz	6.7935	5.2927	5.2593	10.5855
10	2	1.20	0.30	rotated	6.7935	4.5448	4.5389	9.0897
10	2	1.20	0.60	petz	4.2792	3.7692	3.7261	7.5383
10	2	1.20	0.60	rotated	4.2792	3.2002	3.1844	6.4005
10	2	1.20	1.00	petz	2.8631	2.6564	2.6414	5.3128
10	2	1.20	1.00	rotated	2.8631	2.2785	2.2655	4.5570
10	2	1.20	1.50	petz	2.0053	1.9110	1.9159	3.8221
10	2	1.20	1.50	rotated	2.0053	1.6315	1.6266	3.2630
10	2	1.20	2.00	petz	1.5420	1.4693	1.4834	2.9387
10	2	1.20	2.00	rotated	1.5420	1.2423	1.2446	2.4846
10	2	1.50	0.30	petz	6.3827	5.1851	5.1450	10.3701
10	2	1.50	0.30	rotated	6.3827	4.3791	4.3633	8.7581
10	2	1.50	0.60	petz	3.9869	3.5227	3.4867	7.0453
10	2	1.50	0.60	rotated	3.9869	3.0035	2.9915	6.0071
10	2	1.50	1.00	petz	2.6913	2.4388	2.4213	4.8775
10	2	1.50	1.00	rotated	2.6913	2.0939	2.0766	4.1878
10	2	1.50	1.50	petz	1.9329	1.7097	1.7041	3.4193
10	2	1.50	1.50	rotated	1.9329	1.4609	1.4492	2.9219
10	2	1.50	2.00	petz	1.5391	1.2830	1.2795	2.5659
10	2	1.50	2.00	rotated	1.5391	1.0952	1.0891	2.1904

Table 1: Exponential-fit slopes for $I(A:C|B)$, the trace-distance recovery error T, the Hilbert–Schmidt error, and the lower bound $T^2 \leq 1 - F$ inferred from Fuchs–van de Graaf.

h	β	$w^\star_T$	$w^\star_{\mathrm{HS}}$	$w^\star_{T^2}$
1.05	0.30	3	3	3
1.05	0.60	3	3	3
1.10	0.30	3	3	3
1.10	0.60	3	3	3
1.20	0.30	3	3	3
1.20	0.60	3	3	3
1.50	0.30	3	3	3
1.50	0.60	3	3	3

Table 2: Crossover widths $w^\star$ in cases where rotated-Petz is better at $w = 1$ but Petz overtakes for larger buffer width.